Monoclinic M_1 phase of VO_2: Mott-Hubbard versus band insulator

A. S. Belozerov,* M. A. Korotin, and V. I. Anisimov
Institute of Metal Physics, Russian Academy of Sciences, 620990 Ekaterinburg, Russia

A. I. Poteryaev
Institute of Metal Physics, Russian Academy of Sciences, 620990 Ekaterinburg, Russia and Institute of Quantum Materials Science, 620107 Ekaterinburg, Russia

(Received 16 September 2011; revised manuscript received 20 December 2011; published 12 January 2012)

We revisit the problem of the insulating ground state of the monoclinic M_1 phase in vanadium dioxide and argue that essential intersite correlation effects within vanadium dimers can be captured by the static mean-field approximation. We propose the LDA + DMFT + V approach, which combines the density functional theory within the local density approximation (LDA) with the extended Hubbard model. In this approach, the intersite Coulomb interactions beyond the LDA are taken into account by the Hartree-Fock approximation, while the on-site ones are described by the dynamical mean-field theory (DMFT). The proposed approach as well as the cluster extension of the DMFT are used to study the spectral and magnetic properties of the M_1 phase. According to our results, taking into account intersite correlations in vanadium dimers enhances bonding-antibonding splitting with respect to the LDA one, resulting in an insulating ground state, whereas on-site correlations only slightly change the picture, leading to a renormalization of bands. The magnetic properties of the M_1 phase can be attributed to the singlet ground state of vanadium dimers. We conclude that the M_1 phase is a correlated band insulator and the Peierls scenario, enhanced by the intersite correlation effects, is the driving mechanism of the metal-insulator transition in VO_2.

DOI: 10.1103/PhysRevB.85.045109 PACS number(s): 71.15.Mb, 71.27.+a, 71.30.+h

I. INTRODUCTION

Metal-insulator transitions (MIT) in transition-metal compounds draw a lot of attention due to the accompanying dramatic changes in structural and spectral properties. The driving mechanisms of these transitions as well as the role of correlation effects have been extensively investigated theoretically and experimentally for over half a century.[1] Despite substantial progress in this field, there are a lot of issues which are still eagerly debated. MIT in vanadium dioxide, VO_2, is of great interest owing to application perspectives. Large changes of resistivity and optical properties at almost room temperature allow one to use this material for modern electronics devices, in different optical and electric switches, and, in particular, for so-called intelligent windows.[2] The transition from a high-temperature metallic rutile (R) phase to a low-temperature insulating monoclinic (M_1) phase is observed at 340 K and ambient pressure.[3] The crystal structures of both phases are closely related. While in high symmetry the R phase equidistant vanadium atoms form chains along the c_R axis, a unit cell of the M_1 phase can be regarded as one of the R phase doubled along the c_R axis with dimerization and tilting of vanadium atoms (Fig. 1).

The most intriguing challenge is to determine a scenario of the transition and the role of correlation effects. The first qualitative explanation of the transition was proposed by Goodenough.[4] In Goodenough's picture, dimerization of vanadium atoms in the M_1 phase results in bonding-antibonding splitting. The d electrons occupy the bonding combination leading to a band gap between the bonded and π states. The system becomes nonmagnetic,[5,6] which favors Peierls picture of the transition. A different interpretation was proposed by Rice *et al.*,[7] who pointed out that in another insulating monoclinic phase (M_2), half of the vanadium chains behave as the Heisenberg antiferromagnetic ones with spin 1/2. The temperature dependence of magnetic susceptibility[5] and recent spectroscopy experiments[8,9] for the high-temperature R phase also show that correlation effects are essential.

Conventional band structure calculations[10] do not reveal an insulating behavior of the M_1 phase. It is important to note that for the R phase, the experimentally observed peak[8,9] at -1 eV is not also reproduced by the local density approximation (LDA). Thus, the conventional band structure methods leave the issue of the transition scenario open. The GW calculations allow one to obtain an insulator,[11] but many-body corrections do not much affect the shape and the dispersion of the LDA energy bands, enhancing the separation of the V 3d bands into bonding and antibonding subbands. In the recent work of Eyert,[12] vanadium dioxide was investigated using the hybrid density functional,[13] which combines the nonlocal Hartree-Fock expression with the generalized gradient approximation (GGA). In this work, the insulating phases are well described in terms of the band gap and long-range magnetic ordering, while the comparison with spectroscopy and magnetic experimental data for the R phase is less satisfactory. The account of strong electron correlations was done in the calculations[14,15] by the LDA + DMFT method, which combines the LDA and dynamical mean-field theory (DMFT), and it was shown that the short-range spacial correlations are essential for a proper description of the M_1 physics.[16,17] Hence, most of the computational results show the importance of spacial intradimer (as minimum) correlations for the low-temperature M_1 phase.

The intersite Coulomb interactions simultaneously with on-site ones in first-principles calculations have been taken into account in Ref. 18. Recently, the DFT + U + V method, which is an extension of the DFT + U approach,[19] has been

proposed.[20] In this method, extra terms corresponding to the on-site and intersite Coulomb interactions are added to the density functional theory (DFT) functional. It has been shown[20,21] that including intersite Coulomb interactions is important for systems where hybridization between orbitals centered on different sites plays a significant role. This is especially relevant for highly covalent transition-metal compounds and, in particular, for VO_2.

In this work, we go one step further and propose the LDA + DMFT + V approach (although the LDA is used for the notation, the GGA is also valid). In this scheme, the material specific aspects come from the band structure calculations; the strong on-site electron-electron correlations are treated with use of the DMFT, while the intersite Coulomb interactions, poorly described in the above-mentioned approximations, are regarded in the static mean-field way. Therefore, this method allows one to describe spacial correlations missed in the conventional single-site LDA + DMFT and is an order of magnitude faster than any available extension of DMFT that considers spacial degrees of freedom. The proposed approach as well as the cluster DMFT[22] (CDMFT) was used in the present work to study the spectral and magnetic properties of the M_1 phase of vanadium dioxide. The detailed analysis of the CDMFT results validate the applicability of the LDA + DMFT + V method. It is demonstrated that essential intersite correlation effects within vanadium dimers can be captured by the static mean-field approximation, and the insulating ground state of the M_1 phase can be properly described.

We conclude that the M_1 phase of VO_2 is a correlated band insulator and the Peierls scenario, enhanced by the intersite correlation effects, is the driving mechanism of the MIT in vanadium dioxide. This paper is organized as follows. In Sec. II, the extended Hubbard model and DFT within the LDA are combined in the LDA + DMFT + V method. In Sec. III, the spectral and magnetic properties of the M_1 phase are studied. The obtained results are compared with those of previous calculations and experimental data. In Sec. IV, the conclusions and perspectives are discussed.

II. METHOD

The Hubbard model,[23] due to its simplicity and sound physical principles, has become one of the most important models and a powerful tool in the theory of strongly correlated electron system. It has been extensively used in many-body systems studied by means of both model Hamiltonians with adjustable parameters and the first-principles methods. In the latter case, employing the Hubbard model resulted in the LDA + U (Ref. 19) and more sophisticated LDA + DMFT[24,25] methods, which have been introduced in order to improve the description of Mott localizations.

The Hubbard model supplemented by the nearest-neighbor interactions is usually referred to as the *extended Hubbard model*[26] (EHM), and its Hamiltonian reads as

$$\hat{H}_{\mathrm{EHM}} = \hat{H}_t + \hat{H}_U + \hat{H}_V, \tag{1}$$

where the first term represents a kinetic-energy part, while the last two are on-site and intersite interaction terms, respectively. These terms, written in the second quantization notations (for simplicity, angular momentum quantum numbers will be omitted), have the form

$$\hat{H}_t = -\sum_{\langle i,j\rangle}\sum_{\{m\},\sigma} t^{ij}_{mm'}(\hat{c}^+_{im\sigma}\hat{c}_{jm'\sigma} + \mathrm{H.c.}), \tag{2}$$

$$\hat{H}_U = \frac{1}{2}\sum_i \sum_{\substack{\{m\}\\ \sigma,\sigma'}} V^{ii}_{mm'm''m'''}\hat{c}^+_{im\sigma}\hat{c}^+_{im'\sigma'}\hat{c}_{im'''\sigma'}\hat{c}_{im''\sigma}, \tag{3}$$

$$\hat{H}_V = \frac{1}{2}\sum_{\langle i,j\rangle} \sum_{\substack{\{m\}\\ \sigma,\sigma'}} V^{ij}_{mm'm''m'''}\hat{c}^+_{im\sigma}\hat{c}^+_{jm'\sigma'}\hat{c}_{jm'''\sigma'}\hat{c}_{im''\sigma}, \tag{4}$$

where $\hat{c}^+_{im\sigma}$ ($\hat{c}_{im\sigma}$) denotes the creation (annihilation) operator of an electron with spin σ ($=\uparrow,\downarrow$) at the orbital m of the site i; $t^{ij}_{mm'}$ is the hopping matrix element, and $V^{ij}_{mm'm''m'''} \equiv \langle im, jm'|\hat{V}_{ee}|im'', jm'''\rangle$ is the matrix element of the Coulomb interaction between sites i and j ($\hat{V}_{ee}$ is the operator of the screened Coulomb interaction). The sum over $\langle i,j\rangle$ means the summation over all nearest-neighbor sites, and $\{m\}$ denotes the set of magnetic quantum numbers. Being a simple generalization of the Hubbard model, the EHM has been extensively used to investigate electron-correlation phenomena in solids. In many cases, an interplay between on-site and intersite interactions has been shown to be important,[27] leading to a charge density wave or antiferromagnetic order. Special attention has been attracted to the high-temperature superconductors, where the role of intersite interactions is still under debate.[28]

In order to improve the description of the systems where on-site and intersite interactions are significant, we combine the DFT within the LDA and EHM in the LDA + DMFT + V method, standing as a powerful tool for calculations in an *ab initio* manner. In this method, the hopping integrals of Eq. (2) are calculated by the DFT,[24,29] the on-site Coulomb interaction term [Eq. (3)] is considered in a precise way by the DMFT, and the intersite Coulomb interaction term [Eq. (4)] is treated in the static Hartree-Fock-like approximation. In the framework of the DMFT, a lattice problem with many degrees of freedom is mapped to the quantum impurity embedded in the time-dependent self-consistent bath. The detailed description of the DMFT methods can be found in many sources,[30] and here we will focus only on the inclusion of the intersite contribution.

Let us consider Eq. (4) corresponding to the intersite term of the EHM. By means of the static mean-field approximation,[31] one can decouple the four-operator term,

$$\begin{aligned}&\hat{c}^+_{im\sigma}\hat{c}^+_{jm'\sigma'}\hat{c}_{jm'''\sigma'}\hat{c}_{im''\sigma}\\ &\quad\Rightarrow \langle\hat{c}^+_{im\sigma}\hat{c}_{im''\sigma}\rangle\hat{c}^+_{jm'\sigma'}\hat{c}_{jm'''\sigma'} + \langle\hat{c}^+_{jm'\sigma'}\hat{c}_{jm'''\sigma'}\rangle\hat{c}^+_{im\sigma}\hat{c}_{im''\sigma}\\ &\quad-\langle\hat{c}^+_{im\sigma}\hat{c}_{jm'''\sigma'}\rangle\hat{c}^+_{jm'\sigma'}\hat{c}_{im''\sigma} - \langle\hat{c}^+_{jm'\sigma'}\hat{c}_{im''\sigma}\rangle\hat{c}^+_{im\sigma}\hat{c}_{jm'''\sigma'}.\end{aligned} \tag{5}$$

Assuming collinear magnetic order and introducing an occupation matrix in the following form:

$$n^{ij}_{m'm''\sigma} = \langle\hat{c}^+_{im'\sigma}\hat{c}_{jm''\sigma}\rangle, \tag{6}$$

the intersite term [Eq. (4)] can be expressed in the single-particle form,

$$\hat{H}_V = \sum_{\langle i,j\rangle}\sum_{\{m\},\sigma} V^{ij}_{mm'm''m'''}\left(n^i_{mm''}\hat{n}^j_{m'm'''\sigma} - n^{ij}_{mm'''\sigma}\hat{c}^+_{jm'\sigma}\hat{c}_{im''\sigma}\right), \tag{7}$$

where $n^i_{mm''} = n^{ii}_{mm''\sigma} + n^{ii}_{mm''\bar{\sigma}}$. One should notice that the first term in this equation corresponds to the purely electrostatic Coulomb interaction between nearest-neighbor sites, while the last modifies the hopping amplitudes.

Merging the DFT and EHM, one should subtract the Coulomb contribution from the exchange-correlation potential to avoid double counting of the Coulomb interaction. Unfortunately, there is no rigorous way to do this because the Coulomb interaction energy in the framework of DFT is calculated as a functional of the charge density. In the case of an on-site interaction, different approaches to the choice of the double-counting correction have been proposed and studied.[32] Following these ideas, it is reasonable to assume that the LDA exchange-correlation potential, being approximated by that of the homogeneous electron gas, accurately captures electrostatic Coulomb interactions between different sites in some averaged sense, while the effects, caused by strong hybridization between orbitals centered on neighbor sites, are missed. This eliminates the first term in Eq. (7), resulting in the single-particle Hamiltonian,

$$\hat{H}_{\mathrm{LDA}+V} = \hat{H}_{\mathrm{LDA}} - \sum_{\langle i,j\rangle}\sum_{\{m\},\sigma} V^{ij}_{mm'm''m'''} n^{ij}_{mm'''\sigma}\hat{c}^+_{jm'\sigma}\hat{c}_{im''\sigma}. \tag{8}$$

As shown by Campo and Cococcioni,[20] the same result can also be obtained by variation of the functional

$$E_{\mathrm{LDA}+V}[\rho(\mathbf{r}),\{n\}] = E_{\mathrm{LDA}}[\rho(\mathbf{r})] + E_V[\{n\}] - E_{\mathrm{dc}}[\{n\}], \tag{9}$$

where

$$E_V[\{n\}] = \frac{1}{2}\sum_{\langle i,j\rangle} V^{ij}\left[n^i n^j - \sum_{\sigma}\mathrm{Tr}\left(n^{ij}_{\sigma} n^{ji}_{\sigma}\right)\right], \tag{10}$$

$$E_{\mathrm{dc}}[\{n\}] = \frac{1}{2}\sum_{\langle i,j\rangle} V^{ij} n^i n^j. \tag{11}$$

In these equations, $\rho(\mathbf{r})$ is the charge density, $E_{\mathrm{LDA}}[\rho(\mathbf{r})]$ is the LDA functional, $E_V[\{n\}]$ and $E_{\mathrm{dc}}[\{n\}]$ correspond to the intersite Hubbard-like functional and double-counting correction, respectively, and the trace operator indicates the sum over the diagonal elements of the matrix it acts on, $\mathrm{Tr}\{O\} = \sum_m O_{mm}$. Thereby, the contribution of the corrective functional to the Kohn-Sham potential can be expressed as

$$\hat{V}^{\sigma}\left|\psi^{\sigma}_{kv}\right\rangle = \frac{\delta E_V}{\delta(\psi^{\sigma}_{kv})^*} = -\sum_{\langle i,j\rangle}\sum_{\{m\}} V^{ij}_{mm'm''m'''} n^{ij}_{mm'''\sigma}\left|\phi^j_{m'}\right\rangle\left\langle\phi^i_{m''}\right|\left.\psi^{\sigma}_{kv}\right\rangle, \tag{12}$$

where $|\phi^j_{m'}\rangle$ are the localized orthonormal orbitals, and $|\psi^{\sigma}_{kv}\rangle$ are the Kohn-Sham orbitals.

Hence, one may conclude that the LDA underestimates the coupling tendency between states from neighbor sites, as well as the tendency to the localization of electrons. Accurate treatment of the intersite interactions is of great importance when the hybridization between orbitals centered on different sites is essential (e.g., formation of the molecular orbitals). Special attention should be given to the compounds where the electrons are localized on the states belonging to several sites. One of them is the insulating M_1 phase of VO_2. As it will be shown in Sec. III, in this case the LDA underestimates the bonding-antibonding energy splitting, and taking into account intersite interactions plays an important role.

The above equations can be easily extended to the case when interactions between different manifolds are also considered. However, taking into account multiple interactions is quite tedious and it is reasonable to consider only the most relevant ones. In contrast to the on-site interaction that may be parametrized by two parameters (U and J) for the spherically symmetric case, there is no universal parametrization for the intersite interaction matrix $V^{ij}_{mm'm''m'''}$ (however, crystal symmetry can be used for this). To find these values, one may employ the same methods which are widely used for calculation of the on-site interaction parameters, like constrained DFT[33] or constrained random-phase approximation.[34] Hence, we are able to construct the LDA + DMFT + V scheme without adjustable parameters and keep its high predictive power. At the same time, since the proposed method is much cheaper than the LDA + CDMFT, the variation of the interaction parameters allows for numerical experiments and the study of the different energy scales, like in the model approaches.

It is important to notice that when joining the DFT and model Hamiltonian approach, one should be careful with the choice of the exchange-correlation potential because each approach captures the interaction energy in a different way. The double-counting correction introduced above corresponds to the mean-field approximation of the many-body problem and may be used with the LDA and GGA.

III. RESULTS AND DISCUSSIONS

A. Crystal structure and LDA results

In the low-temperature M_1 phase, below 340 K, vanadium dioxide has a monoclinic crystal structure with space group $P2_1/c$ (details can be found in Ref. 35). This structure is presented in Fig. 1 and can be viewed as a distorted high-symmetry rutile structure doubled along the c_R axis (c axis of R phase). There is one type of vanadium atoms that shift to each other, forming dimers tilted with respect to the c_R direction. The dimerized pairs of atoms are connected by green tubes in Fig. 1 and the tilting is presented by the top view of the structure. Reduction of the crystal symmetry results in a lifting of the degeneracy presented in the original R phase. Each vanadium atom is surrounded by an oxygen octahedron resulting in a splitting of the d level to triply degenerate t_{2g} and doubly degenerate e^{σ}_g states. Additional tetragonal distortion presented in the structure leads to further lifting of degeneracy of the t_{2g} level to the a_{1g}, π_1, and π_2 states ($d_{||}$ and d_{π} according to Goodenough's notations).[4] In the local coordinate system, shown in Fig. 1, by (double) primed axes for the vanadium atom, the local z' axis is chosen to be pointed to the apical oxygen atom, and the local x' and y' are chosen to be pointed to the planar oxygens. Hence, the a_{1g} state

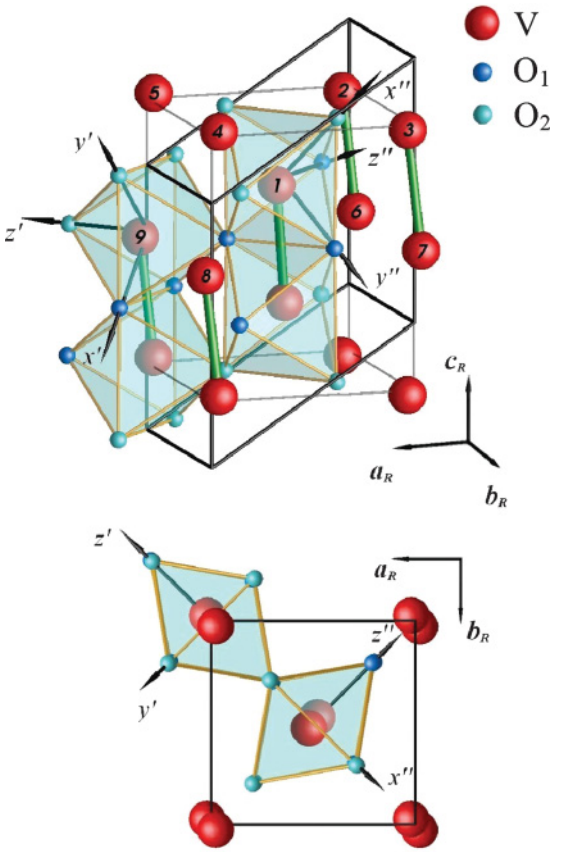

FIG. 1. (Color online) Crystal structure of the monoclinic M_1 phase of VO_2. Vanadium and oxygen atoms are denoted by large (red) and small (blue and cyan) balls. (a_R,b_R,c_R) are rutile crystallographic axes. Local coordinate axes on the vanadium atoms are shown by the (double) primed set. The lower part of the figure shows a lattice top view.

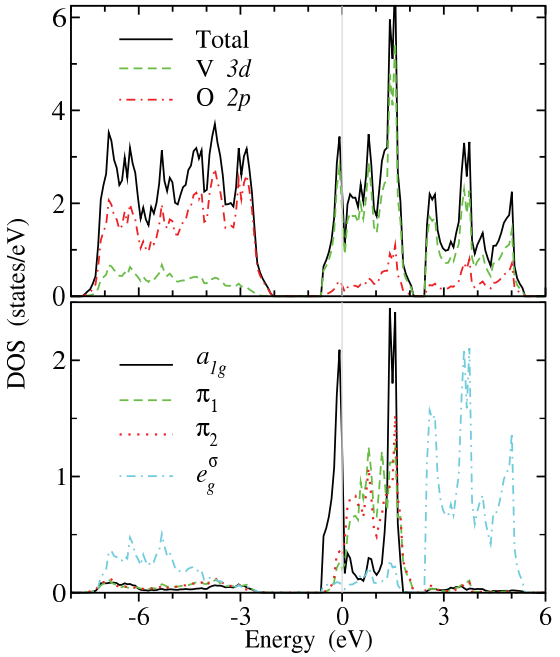

FIG. 2. (Color online) LDA density of states (DOS) for the M_1 phase. Top panel shows total, V $3d$, and O $2p$ DOS's per f.u. by solid (black), dashed (green), and dot-dashed (red) lines, respectively. Bottom panel shows partial DOS's of different symmetry for a vanadium atom. The Fermi level is indicated by the vertical (gray) line at zero energy.

corresponds to the $d_{x'y'}$ orbital, the π states correspond to $d_{x'z'}$ and $d_{y'z'}$, and the e_g^σ states correspond to $d_{z'^2}$ and $d_{x'^2-y'^2}$. This local coordinate system is obtained by rotating to the Euler angles $(\pi/4, -\pi/2, \pi/4)$. The double-primed local coordinate axes are obtained by a proper symmetry operation for the corresponding vanadium atom. It should be noted that the a_{1g} orbitals are parallel to the c_R axis, resulting in a substantial overlap for neighbor vanadium atoms.

In order to calculate the electronic structure of the M_1 phase within the LDA, the tight-binding linear muffin-tin orbital (TB-LMTO) method[36] was used. The obtained results are presented in Fig. 2 and are in good agreement with earlier studies.[10]

As in the case of the R phase,[15] the total density of states (DOS) is divided into three regions. The completely occupied part extends from -8 to -2 eV and is of oxygen character mostly. The middle region, extended from -0.6 to 2.1 eV, crosses the Fermi level and its partial character corresponds to the t_{2g} states of vanadium. The highest energy part of the DOS is separated by a small gap and is located in the energy range from 2.4 to 5.4 eV.

The dimerization of vanadium atoms leads to the well-formed bonding-antibonding structure in the a_{1g} partial DOS, shown in the lower panel of Fig. 2. The bonding states are located just below the Fermi level (and partially cross it), while their antibonding counterparts are at 1.5 eV. The states with π symmetry (averaged $d_{x'z'}$ and $d_{y'z'}$ orbitals shown by dashed line) correspond to the V_d-O_p antibonding states and are shifted upward on approximately 0.3 eV with respect to the R phase, due to the increased overlap of these states with the O states. Hence, the LDA occupations of the orbitals crossing the Fermi level in the M_1 phase differ from those in the R phase. The a_{1g} orbital is occupied by 0.86 electrons and each π orbital is occupied by 0.07 electrons.

The low-energy Hamiltonian for the states near the Fermi level has been constructed with use of the Nth-order muffin-tin orbital (NMTO) method.[37] In order to obtain a Hamiltonian including three bands (V t_{2g} symmetry mainly) for each vanadium atom in the unit cell, the quadratic ($N = 2$) muffin-tin orbital set was used. Hopping integrals for localized functions of different symmetries are presented in Table I. One can immediately see that the intradimer a_{1g}-a_{1g} hopping is the dominant one and defines bonding-antibonding splitting in the density of states. At the same time, the intrachain a_{1g}-a_{1g} hopping from one dimer to another is much smaller and comparable with the rest of the hoppings. The hoppings from the central atom, V_1, to the off-chain atoms are from about 50 to 200 meV. The largest hopping to other distances is smaller than 25 meV. The solution obtained within the LDA is the metallic one, which is in contradiction with the experimental data.[8,9]

B. Spectral properties

The spectral properties of the M_1 phase are characterized by a band gap of about 0.6 eV (Ref. 9). One of the approaches

TABLE I. Hopping integrals (in meV) for d electrons in the M_1 phase. The first column indicates the vanadium atoms according to the notations in Fig. 1. The distances between vanadium atoms are in the second column. The largest hopping to other distances is smaller than 25 meV and not shown here.

	d (Å)		a_{1g}	π_1	π_2
Intradimer		a_{1g}	−734	−7	11
hoppings	2.62	π_1	−7	114	122
		π_2	11	122	131
Intrachain		a_{1g}	−58	−27	19
hoppings	3.17	π_1	−27	19	64
		π_2	19	64	12
1 → 2		a_{1g}	9	−57	36
1 → 9	3.65	π_1	10	−77	−205
		π_2	3	40	41
1 → 4		a_{1g}	25	−10	12
1 → 5	3.48	π_1	−42	44	−116
		π_2	62	27	−232
1 → 6		a_{1g}	−11	−9	23
1 → 7	3.57	π_1	11	22	6
		π_2	1	−172	−95
1 → 3		a_{1g}	−13	−2	−10
1 → 8	3.40	π_1	135	−153	−2
		π_2	−116	−118	18

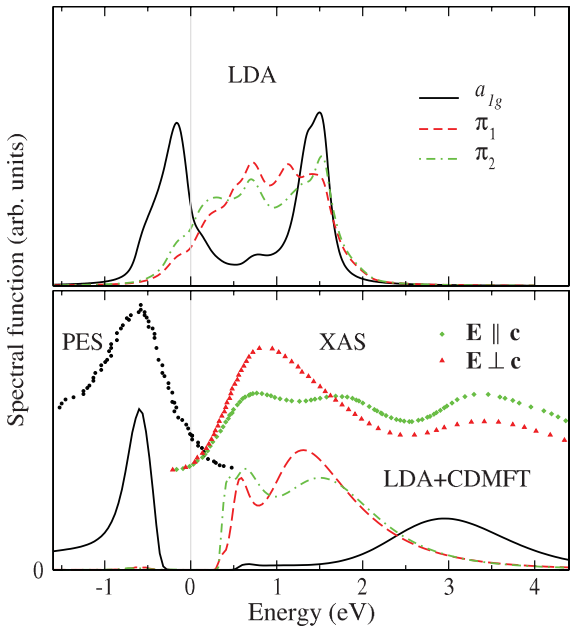

FIG. 3. (Color online) Spectral functions for the M_1 phase calculated by the LDA (upper panel) and LDA + CDMFT (lower panel). The results of photoemission spectroscopy (PES) and O K x-ray absorption spectroscopy (XAS) with different polarization (reproduced from Ref. 9) are presented in the lower panel. The Fermi level is indicated by the vertical (gray) line at zero energy.

that allows one to obtain an insulating solution for the M_1 phase is the GW scheme.[11] Nevertheless, model many-body corrections do not much affect the shape and the dispersion of the energy bands, but only rigidly shift the occupied (unoccupied) a_{1g} states downward (upward) in energy. This enhances the separation of the a_{1g} band into the bonding and antibonding subbands, leading to a bandlike character of the transition. Another approach has been proposed by Eyert.[12] He used the Heyd-Scuseria-Ernzerhof (HSE) hybrid density functional[13] in the framework of the DFT. This hybrid functional combines the nonlocal Hartree-Fock expression with the GGA and can be viewed as a screened Coulomb potential applied only for the exchange interaction in order to screen the long-range part of the Hartree-Fock exchange.

As shown above, the LDA alone fails to reproduce the energy-band gap in the M_1 phase (see Fig. 2). Although taking into account on-site Coulomb interactions by the single-site DMFT approach allows one to correctly describe the R phase,[15,16,38] the insulating ground state of the M_1 phase in this approach can be obtained only with unphysically large values of the on-site interaction parameter ($U \geqslant 6$ eV). This indicates that nonlocal correlation effects, neglected in the single-site DMFT approach, are essential in the M_1 phase. To take into account short-range correlations in vanadium dimers, Biermann *et al.*[16] have employed the cluster extension of the DMFT. In this approach, the vanadium dimer was considered as an impurity in the Anderson model, and hence interdimer self-energy elements were introduced.

In our calculations, we used the value of the screened Coulomb interaction, $U = 4$ eV, and the value of Hund's exchange, $J = 0.68$ eV, from the earlier paper (Ref. 16). This value of the Coulomb interaction is consistent with the other theoretical estimations.[34] We found also that LDA + DMFT + V results depend weakly on the particular choice of U in the range from 3 to 5 eV. For the solution of the quantum impurity problem, the multiorbital Hirsch-Fye quantum Monte Carlo (QMC) method was used.[39] In the QMC calculations, the imaginary time was discretized into L slices so as to keep $\beta/L = 0.25$ eV^{-1} for all temperatures, where β denotes the inverse temperature. Also, QMC steps of the order of 10^6 to 10^7 were used to satisfy ergodicity. The spectral functions obtained by the LDA + CDMFT approach at $\beta = 20$ eV^{-1} are presented in the lower panel of Fig. 3. One can see that the bonding and antibonding states from the LDA (upper panel of Fig. 3) are transformed to the narrow peak below the Fermi level at about −0.7 eV and the broad states spread from 0.5 to 4.5 eV, respectively. The former is clearly seen in the photoemission spectroscopy (PES) data[9] (reproduced in Fig. 3 by black dots), while the latter centered at 3 eV can be compared with the polarization-dependent O K x-ray absorption spectroscopy (XAS) results[9] (reproduced in Fig. 3 by green diamonds and red triangles). Here, the XAS measurements are used to investigate conduction bands and correspond to the transitions from the O 1s to the O 2p states, which are mixed with the unoccupied V 3d ones. The polarization vector **E** was pointed parallel (green diamonds) and perpendicularly (red triangles) to the crystallographic axis **c**. The first peaks above the Fermi level at the XAS spectra can be attributed to the π states, while the strong polarization dependence suggests that the middle peak, observed only when **E**⊥**c**, indicates the a_{1g} states. Though the position of the a_{1g} antibonding states in the CDMFT calculations turns out to be shifted to higher energies with respect to the XAS measurements, the value of the band gap of about 0.5 to 0.6 eV between bonding a_{1g} and π states is in agreement

with the experimental data.[9] It is important to note that the obtained splitting between the bonding and antibonding states is considerably enhanced compared to that from the LDA (1.5 and 3.5 eV, respectively).

Relying on the CDMFT results, Tomczak *et al.*[38,40] have proposed an effective band structure for the M_1 phase, based on the finding that self-energies in physically meaningful energy domains are almost energy independent. They constructed an orbital-dependent static one-particle potential that reproduces the essentials of the full many-body spectrum. It is necessary always to keep in mind that the DFT is a theory of a ground state only, not of excited states. Therefore, the energy spectrum has no precise physical meaning in the framework of the DFT. According to this, the proposed correction to the LDA band structure seems to be quite reasonable. In order to stress the main qualitative results of these authors, we would like to revisit this effective band structure. In contrast to these authors, we used Pade approximants[41] for analytic continuation of the self-energies to the real energy domain. Neglecting lifetime effects, the excitation energies can be determined as the poles of the one-particle Green function (for more details, see Refs. 38 and 40). This results in the quasiparticle equation and its qualitative solutions can be obtained graphically. The solutions are the intersections of the self-energy real part with a frequency stripe of slope one and a width corresponding to the dispersion of the LDA band. The real parts of the obtained self-energies for the bonding and antibonding states are presented in Fig. 4 (chemical potential was subtracted).

Despite some discrepancies, our results are in agreement with those of the above-mentioned authors in relevant regions. In order to indicate these regions, gray stripes corresponding to the LDA bonding and antibonding states are presented in Fig. 4. One can see that the real parts of the self-energies only weakly depend on energy in these domains, resulting mainly in an increase of the bonding-antibonding energy splitting. The shifting of the π states with respect to the a_{1g} ones turns out to be less than 0.1 eV and can be neglected as a minor effect. According to this, one of the main effects of employing CDMFT is the renormalization of the effective intradimer hopping, resulting in the opening of a band gap.

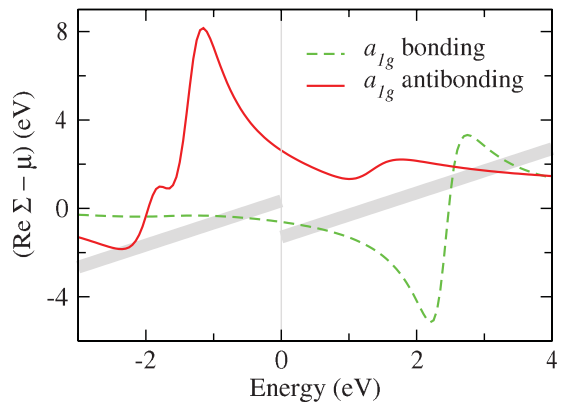

FIG. 4. (Color online) Real parts of the bonding (solid red line) and antibonding (dashed green line) self-energies (chemical potential was subtracted) calculated by the LDA + CDMFT. The gray stripes represent the extent of the LDA bands (see text for a discussion).

Let us consider taking into account intersite Coulomb interactions in the M_1 phase in the framework of the LDA $+V$ approach. As stressed in Sec. II, the LDA underestimates the coupling tendency between orbitals centered on neighbor sites and this effect is proportional to the value of the intersite occupation. Based on the LDA results, one can conclude that intersite occupations for all orbitals, except that of a_{1g} symmetry, are negligibly small, which significantly simplifies the problem and allows one to consider only the intersite interactions between a_{1g} orbitals. Then the intersite Coulomb interaction matrix is reduced to the scalar, $V^{ij}_{mm'm''m'''} = V$. In this case, the value of intersite interaction strength, $V = 2$ eV,[42] is close to that in other transition-metal dioxides[21] and to the value obtained for $SrVO_3$ where vanadium-vanadium bonding is much weaker.[34] The orbitally resolved spectral function obtained by the LDA $+V$ calculation is presented in the upper panel of Fig. 5. One can see that the almost-fully-occupied bonding states are pushed down in energy by $V/2$, while the empty antibonding states are pushed up by $V/2$, resulting in a gap of about 0.7 to 0.8 eV between bonding a_{1g} and π states. The band gap opens at $V = 0.9$ eV and depends almost linearly on V according to Eq. (7). Hence, taking into account intersite correlations only turns out to be sufficient to obtain an insulating solution for the M_1 phase. Nevertheless, the ground state is beyond a static one-particle description, and, in order to take into account on-site electron-electron correlations in the partially filled d band, we use the single-site DMFT method. The obtained orbitally resolved spectral functions are presented in the lower panel of Fig. 5. One can see that

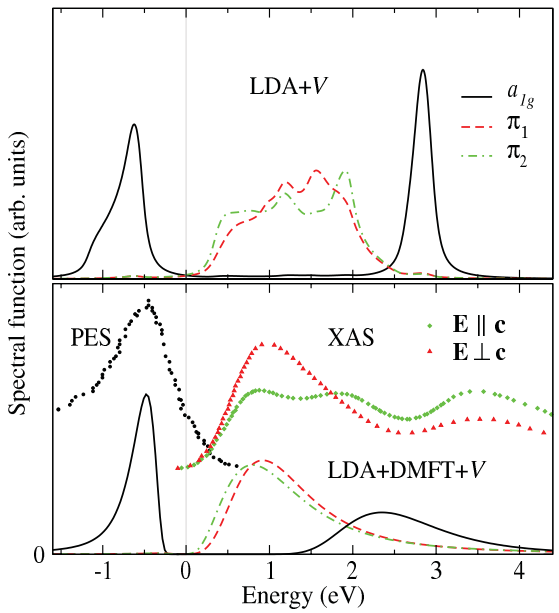

FIG. 5. (Color online) Spectral functions for the M_1 phase calculated by the LDA $+V$ (upper panel) and LDA + DMFT $+V$ (lower panel). The results of photoemission spectroscopy (PES) and O K x-ray absorption spectroscopy (XAS) with different polarization (reproduced from Ref. 9) are presented in the lower panel. The Fermi level is indicated by the vertical (gray) line at zero energy.

the on-site Coulomb correlations only slightly change the picture obtained by the LDA $+V$ calculations, leading to a renormalization of bands. This is in agreement with the results of the previous studies of correlations in band insulators.[43] Besides, the charge gap is correctly opened and the spectral functions agree well with the experimental data. The bonding-antibonding splitting turns out to be renormalized by the on-site electron correlations and is about 3.0 eV.

One can see that the results obtained by the LDA + DMFT $+V$ and LDA + CDMFT are in agreement with each other. This can be easily explained in the following way: Taking into account intersite Coulomb correlations in the mean-field approximation corresponds to the static (energy-independent) intersite self-energy elements, which resemble the ones obtained by the CDMFT. As one can see in Fig. 4, the self-energy corresponding to bonding a_{1g} states (dashed line) is nearly energy independent in the energy region around the Fermi level. In fact, the CDMFT provides a way for inclusion of the intersite interactions, but the use of this approach is limited to the cases when a simple cluster can be easily introduced according to the physical reasons. In more sophisticated cases, when an elementary cluster includes many sites or orbitals, calculations require significant computational resources and very often cannot be put into practice. Moreover, one should keep in mind that the CDMFT breaks translational invariance, because the components of self-energy within the cluster are kept, but not the components between clusters. Thereby, the proposed LDA + DMFT $+V$ method is the next step forward toward the combination of the DFT and model Hamiltonian approach into a powerful tool for the description of the strongly correlated electron system.

In order to describe the spectral properties of the M_1 phase more accurately, it is necessary to take into account quite strong hybridization between the V $3d$ and O $2p$ states and use the "full" basis including these states for the DMFT calculations. In this case, in addition to the correlated states, the uncorrelated ones appear in the low-energy Hamiltonian and a double-counting correction for the on-site interaction has to be introduced. This allows one to compare the obtained spectral functions, which include both V $3d$ and O $2p$ states, with the experimental ones in a more accurate manner. These activities are already in progress and results will be presented elsewhere.

C. Magnetic properties

The metal-insulator transition in VO_2 is accompanied by substantial changes in magnetic properties. According to the experimental data,[5,6] the M_1 phase of stoichiometric VO_2 has a temperature-independent Van Vleck paramagnetic susceptibility of about 6.5×10^{-5} emu/mole. This is in contrast with the metallic R phase, where uniform magnetic susceptibility obeys the Curie-Weiss law with the effective local magnetic moments formed by vanadium d electrons.[5,15] The nuclear magnetic resonance (NMR) measurements[44] indicate the absence of magnetic order in the M_1 phase, suggesting that it does *not* belong to the classical Mott-Hubbard insulators, where on-site Coulomb repulsion leads to the formation of local magnetic moments. This fact favors the band picture, where electrons localize on molecular orbitals of vanadium pairs. However, two other insulating phases called M_2 and M_3 (also called T phase) have been discovered[45] below the transition temperature (T_{MI}). These phases can be obtained by small doping[44] or uniaxial stress[46] applied in the $[110]_R$ direction in pure VO_2. In the monoclinic M_2 phase, there are two types of vanadium chains. One-half of the chains is formed by dimerized V atoms, which, in contrast to those in the M_1 phase, are not tilted with respect to the chains direction. The other half consists of equidistant V atoms, which are tilted due to electrostatic forces and form zigzags. The NMR[44,47] and electron paramagnetic resonance[48] experiments found the formation of the local magnetic moments on atoms of the zigzags chains, suggesting that these chains should be attributed to the Mott-Hubbard type. Pouget *et al.*[44] have shown that these zigzag chains can be described in terms of the noninteracting linear Heisenberg chains with spin $S = 1/2$ and concluded that all insulating phases of VO_2 should be regarded as Mott-Hubbard insulators. Thus, the detailed analysis of the magnetic properties of the M_1 phase turns out to be significant to understand the underlying physics and provides a way to verify the validity of the approaches used.

Following the linear response idea, the uniform magnetic susceptibility can be calculated directly in the DMFT by adding to the Hamiltonian a term that corresponds to the interaction with the external magnetic field H_z, and measuring the magnetization of the compound. Then, the uniform magnetic susceptibility can be defined as

$$\chi(T) = \frac{m(T)}{H_z}, \tag{13}$$

where $m(T) = \sum_m n_m^{\uparrow} - n_m^{\downarrow}$ is the magnetization at the given temperature. A few magnetic fields in the range from 0.02 to 0.1 eV were used to check and satisfy the condition of response linearity. The uniform magnetic susceptibilities of the M_1 phase calculated by different approaches, as well as the experimental temperature-independent value,[5] are shown in Fig. 6. Due to the dominance of the crystal-field effects upon the temperature effects and computational costs of the QMC method at low temperatures, the calculations were performed in the vicinity of T_{MI} and slightly above it. One can clearly see

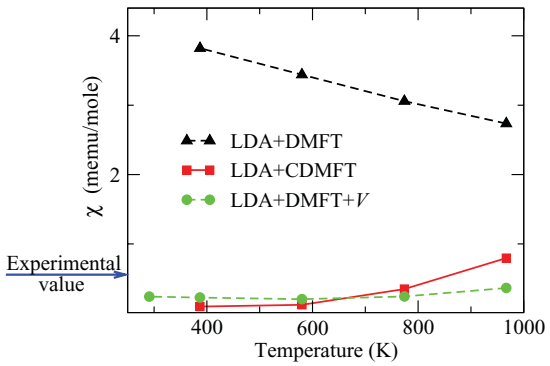

FIG. 6. (Color online) Uniform magnetic susceptibilities for the M_1 phase. The LDA + DMFT results are shown by black triangles, the LDA + CDMFT by red squares, and the LDA + DMFT $+V$ by green circles; the temperature-independent experimental value from Ref. 5 is indicated by the blue arrow.

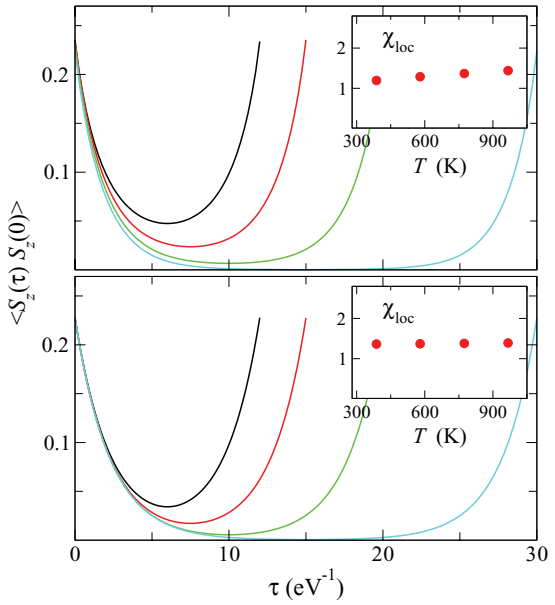

FIG. 7. (Color online) Local spin-spin correlation functions in imaginary-time domain obtained by the LDA + CDMFT for the M_1 phase (upper panel) and calculated exactly for the single-band Hubbard dimer at half-filling with parameters corresponding to the M_1 phase (lower panel). Insets: the temperature dependences of the local spin susceptibilities.

that the conventional single-site DMFT approach shows strong temperature dependence of the uniform magnetic susceptibility which resembles the Curie-Weiss law. This corresponds to the formation of effective local magnetic moments and contradicts the experimental results.[5,6] Both the LDA + CDMFT and LDA + DMFT + V have found the uniform magnetic susceptibility to be almost temperature independent nearby T_{MI}, leading to a qualitative agreement with the experimental data. A quantitative agreement is *not* observed because the deformation effects of electron shells by the external magnetic field, resulting in the Van Vleck paramagnetic susceptibility, were *not* taken into account in the calculations. We would like to stress that the LDA + DMFT + V allows one to calculate at a lower temperature than the LDA + CDMFT at the same computational costs.

We have also calculated the local spin-spin correlation functions $\langle S^z(\tau)S^z(0)\rangle$, which are shown in Fig. 7. Although these functions are pure local quantities and cannot be directly compared to the experimental data, they give a sound source of information about the magnetic properties of the system. The imaginary-time dependences of these correlation functions indicate the time scales of local moment "living" on a site. In the case of strong electron correlations, these functions are expected to depend weakly on the imaginary time, while for the weak Coulomb correlations, they should vary rapidly. The local spin susceptibility can be defined as

$$\chi_{\rm loc} = \frac{g_s^2}{3}\int_0^\beta d\tau\, \langle \mathbf{S}(\tau)\mathbf{S}(0)\rangle. \qquad (14)$$

Here, $g_s = 2$ is the electron-spin g factor, $\mathbf{S}$ is the spin operator on a site, and β is the inverse temperature. In contrast to the uniform magnetic susceptibility, the local spin susceptibility does *not* include the spin polarization of the impurity Weiss field. From the spin-spin correlation functions presented in Fig. 7, one can conclude that at low temperatures, the local-moment lifetimes are small, indicating the nonmagnetic ground state of the M_1 phase. The almost-temperature-independent local spin susceptibility (see the inset on the upper panel in Fig. 7) is in agreement with the previous observation and confirms the absence of localized moments on the sites.

In order to reveal the M_1 physics, let us consider a simple model consisting of the isolated single-band Hubbard dimers. Each of these dimers consists of two sites with the single-particle hopping t between them, and with Coulomb repulsion U for electrons being on the same site. As already shown,[38,44] this simple system at half-filling serves as a quite reliable model for description of the M_1 phase. Besides, due to its simplicity, this problem can be solved exactly. The ground state is a singlet with energy $E_s^- = U/2 - \sqrt{(U/2)^2 + 4t^2}$. It is given by

$$|\psi_{\rm GS}\rangle = \frac{\sin\theta}{\sqrt{2}}(|\uparrow,\downarrow\rangle + |\downarrow,\uparrow\rangle) + \frac{\cos\theta}{\sqrt{2}}(|\uparrow\downarrow,0\rangle + |0,\uparrow\downarrow\rangle), \qquad (15)$$

where θ can be defined as

$$\tan\theta = -\frac{2t}{E_s^-} = \frac{4t}{\sqrt{U^2+16t^2}-U}. \qquad (16)$$

The first excited state is a triplet placed at $E_t = 0$. The second and third excited states are singlets with energy $E_s = U$ and $E_s^+ = U/2 + \sqrt{(U/2)^2 + 4t^2}$, respectively. The dependences of these energy eigenvalues and $\tan^2\theta$ on the U/t ratio are presented in Fig. 8. In the noninteracting limit, the triplet state is above the singlet ground one on $2t$. The latter is characterized by a single Slater determinant. As the U/t ratio increases, the ground state acquires many-body features (i.e., $|\uparrow,\downarrow\rangle$ and $|\downarrow,\uparrow\rangle$ states become more favorable) and the energy required to promote an electron to the first exited state decreases. In the Heitler-London (correlated) limit $U \gg t$, the states with a doubly occupied site are almost projected out, while the

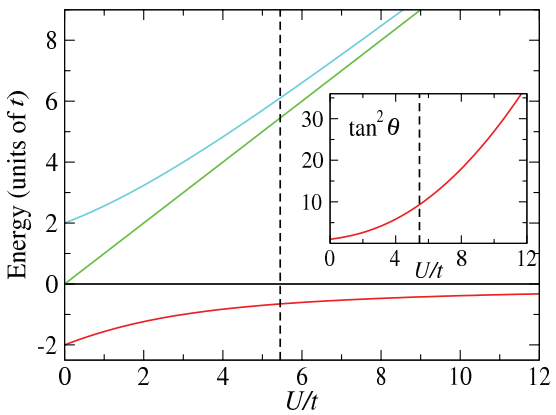

FIG. 8. (Color online) Energy levels of the Hubbard dimer at half-filling. The inset shows the dependence of $\tan^2\theta$ on the U/t ratio. The dashed vertical lines indicate $U/t = 5.45$, corresponding to the parameters of the M_1 phase.

singlet-triplet splitting is substantially reduced with respect to the noninteracting case and can be approximated by $J' = 4t^2/U$. In this limit, the charge fluctuations are almost frozen and only the spins of electrons can fluctuate, thereby reducing the physics of the system to the spin physics described by the so-called $t - J$ model.[49] In Fig. 8, the dashed vertical lines indicate $U/t = 5.45$, corresponding to the parameters of the M_1 phase. Although the system with these parameters is in an intermediate regime, the probability for electrons to be observed on the different sites is about nine times larger than the double-occupation case. Thus, it can be inferred that the correlation effects in this case are essential and the ground state is close to the Heitler-London limit.

At zero temperature, this model system is completely in the singlet ground state and hence nonmagnetic. At higher temperatures, the triplet states are admixed to the ground state, resulting in some magnetic response on the external magnetic field. The spin-spin correlation functions for this system at low temperatures are presented in Fig. 7. One can see that they resemble the ones for the M_1 phase, confirming that the considered system is a reliable model for the M_1 phase. The molar magnetic susceptibility for this system can be expressed as

$$\chi_{\text{mol}} = \frac{4\, g_s^2 \mu_B^2 S^2 N_A \beta}{3 + e^{-\beta E_s^-} + e^{-\beta E_s} + e^{-\beta E_s^+}}, \qquad (17)$$

where μ_B is the Bohr magneton, $S = 1/2$ is the spin quantum number, and N_A is the Avogadro constant. The temperature dependencies of the uniform magnetic and local spin susceptibilities for the set of isolated Hubbard dimers at half-filling with parameters corresponding to the M_1 phase are shown in Fig. 9. One can clearly see that at low temperatures, including the temperature range for the M_1 phase, both curves are almost temperature independent and the system is nonmagnetic. The fact that the values of local spin susceptibility at low temperatures are much larger than that of the uniform magnetic one arises from the different physical quantities they represent. The uniform magnetic susceptibility characterizes the magnetic response of a system on the external magnetic field, whereas the local spin one represents the local spin dynamics. As the temperature increases, the breaking of the covalent bond and formation of the local magnetic moments can be observed. From the linear behavior of the inverse magnetic susceptibilities at high temperatures (see the inset in Fig. 9), one can conclude that both curves are in agreement with each other and represent the Curie-Weiss law.

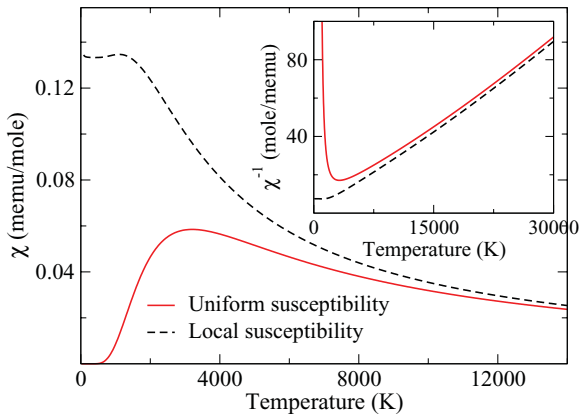

FIG. 9. (Color online) Uniform magnetic (solid red line) and local spin (dashed black line) susceptibilities for the set of isolated single-band Hubbard dimers at half-filling with parameters corresponding to the M_1 phase. Inset: temperature dependences of the inverse susceptibilities.

We conclude that the magnetic properties of the M_1 phase are correctly described by both the LDA + CDMFT and LDA + DMFT + V approaches. The simple model consisting of the isolated single-band Hubbard dimers indicates that the nonmagnetic ground state can be attributed to the singlet states of vanadium dimers.

IV. CONCLUSIONS AND PERSPECTIVES

We have studied the spectral and magnetic properties of the insulating M_1 phase of VO_2 and demonstrated that essential intersite correlation effects within vanadium dimers can be captured by the static mean-field approximation in the framework of the proposed LDA + DMFT + V approach. This approach combines the material specific aspects within the DFT with the extended Hubbard model and allows one to correctly describe the insulating ground state of the M_1 phase. The obtained results are in agreement with the experimental data and allow one to conclude that intersite correlations in vanadium dimers enhance bonding-antibonding splitting with respect to the LDA one, resulting in an insulating solution, whereas on-site correlations lead to a renormalization of bands. Hence, the M_1 phase belongs to the correlated band insulators class and the Peierls scenario, enhanced by the intersite correlation effects, is the driving mechanism of the MIT in VO_2. We have also demonstrated that the vanadium dimers are the key units for a correct description of the magnetic properties of the M_1 phase. The nonmagnetic ground state can be attributed to the singlet states of vanadium dimers.

The LDA + DMFT + V approach can also be applied to other highly covalent transition-metal compounds where hybridization between orbitals centered on different sites plays an important role. Thus, the proposed approach can be considered as a powerful tool for calculations in an *ab initio* manner and may help shed light on some important issues. The detailed analysis of the spectral and magnetic properties of other vanadium dioxide phases will be the subject of our further research.

ACKNOWLEDGMENTS

The authors thank S. Biermann, A. Lichtenstein, and A. Georges, who were at the initial stage of this work,[16] and are grateful to Dm. Korotin and A. Katanin for useful discussions. This work was supported by the Russian Foundation for Basic Research (Projects No. 10-02-00046a, No. 10-02-00546a, and No. 10-02-96011ural), the Dynasty Foundation, the fund of the President of the Russian Federation for the support of scientific schools (Project No. NSH 4711.2010.2), and the Program of the Russian Academy of Science Presidium "Quantum Microphysics of Condensed Matter."

*alexander.s.belozerov@gmail.com

[1] M. Imada, A. Fujimori, and Y. Tokura, Rev. Mod. Phys. **70**, 1039 (1998).

[2] E. E. Chain, Appl. Opt. **30**, 2782 (1991).

[3] F. J. Morin, Phys. Rev. Lett. **3**, 34 (1959).

[4] J. B. Goodenough, J. Solid State Chem. **3**, 490 (1971).

[5] J. P. Pouget, P. Lederer, D. S. Schreiber, H. Launois, D. Wohlleben, A. Casalot, and G. Villeneuve, J. Phys. Chem. Solids **33**, 1961 (1972).

[6] G. Villeneuve, M. Drillon, P. Hagenmuller, M. Nygren, J. P. Pouget, F. Carmona, and P. Delhaes, J. Phys. C **10**, 3621 (1977).

[7] T. M. Rice, H. Launois, and J. P. Pouget, Phys. Rev. Lett. **73**, 3042 (1994).

[8] K. Okazaki, H. Wadati, A. Fujimori, M. Onoda, Y. Muraoka, and Z. Hiroi, Phys. Rev. B **69**, 165104 (2004).

[9] T. C. Koethe, Z. Hu, M. W. Haverkort, C. Schussler-Langeheine, F. Venturini, N. B. Brookes, O. Tjernberg, W. Reichelt, H. H. Hsieh, H.-J. Lin, C. T. Chen, and L. H. Tjeng, Phys. Rev. Lett. **97**, 116402 (2006).

[10] R. M. Wentzcovitch, W. W. Schulz, and P. B. Allen, Phys. Rev. Lett. **72**, 3389 (1994); M. A. Korotin, N. A. Skorikov, and V. I. Anisimov, Phys. Met. Metallogr. **94**, 17 (2002); V. Eyert, Ann. Phys. **11**, 650 (2002).

[11] A. Continenza, S. Massidda, and M. Posternak, Phys. Rev. B **60**, 15699 (1999); M. Gatti, F. Bruneval, V. Olevano, and L. Reining, Phys. Rev. Lett. **99**, 266402 (2007).

[12] V. Eyert, Phys. Rev. Lett. **107**, 016401 (2011).

[13] J. Heyd, G. E. Scuseria, and M. Ernzerhof, J. Chem. Phys. **118**, 8207 (2003).

[14] A. Liebsch, H. Ishida, and G. Bihlmayer, Phys. Rev. B **71**, 085109 (2005); M. Laad, L. Craco, and E. Müller-Hartmann, Europhys. Lett. **69**, 984 (2005); M. S. Laad, L. Craco, and E. Müller-Hartmann, Phys. Rev. B **73**, 195120 (2006).

[15] A. S. Belozerov, A. I. Poteryaev, and V. I. Anisimov, JETP Lett. **93**, 73 (2011).

[16] S. Biermann, A. Poteryaev, A. I. Lichtenstein, and A. Georges, Phys. Rev. Lett. **94**, 026404 (2005).

[17] B. Lazarovits, K. Kim, K. Haule, and G. Kotliar, Phys. Rev. B **81**, 115117 (2010).

[18] V. I. Anisimov, I. S. Elfimov, N. Hamada, and K. Terakura, Phys. Rev. B **54**, 4387 (1996).

[19] V. I. Anisimov, J. Zaanen, and O. K. Andersen, Phys. Rev. B **44**, 943 (1991); V. I. Anisimov, F. Aryasetiawan, and A. I. Lichtenstein, J. Phys. Condens. Matter **9**, 767 (1997).

[20] Vivaldo Leiria Campo Jr and Matteo Cococcioni, J. Phys. Condens. Matter **22**, 055602 (2010).

[21] Heather J. Kulik and Nicola Marzari, J. Chem. Phys. **134**, 094103 (2011).

[22] A. I. Poteryaev, A. I. Lichtenstein, and G. Kotliar, Phys. Rev. Lett. **93**, 086401 (2004).

[23] J. Hubbard, Proc. R. Soc. London A **276**, 238 (1963).

[24] V. Anisimov, A. Poteryaev, M. Korotin, A. Anokhin, and G. Kotliar, J. Phys. Condens. Matter **9**, 7359 (1997).

[25] A. I. Lichtenstein and M. I. Katsnelson, Phys. Rev. B **57**, 6884 (1998).

[26] J. Hubbard, Proc. R. Soc. London A **285**, 542 (1965); **296**, 82 (1967).

[27] A. L. Tchougreeff and R. Hoffmann, J. Phys. Chem. **96**, 8993 (1992); M. P. Lopez Sancho, M. C. Munoz, and L. Chico, Phys. Rev. B **63**, 165419 (2001); L. Y. Zhu and W. Z. Wang, J. Phys. Condens. Matter **18**, 6273 (2006).

[28] P. A. Lee, N. Nagaosa, and Xiao-Gang Wen, Rev. Mod. Phys. **78**, 17 (2006); E. S. Caixeiro and A. Troper, Phys. Rev. B **82**, 014502 (2010).

[29] F. Lechermann, A. Georges, A. Poteryaev, S. Biermann, M. Posternak, A. Yamasaki, and O. K. Andersen, Phys. Rev. B **74**, 125120 (2006).

[30] A. Georges, G. Kotliar, W. Krauth, and M. J. Rozenberg, Rev. Mod. Phys. **68**, 13 (1996); G. Kotliar, S. Y. Savrasov, K. Haule, V. S. Oudovenko, O. Parcollet, and C. A. Marianetti, *ibid.* **78**, 865 (2006).

[31] A. Fetter and J. Walecka, *Quantum Theory of Many-Particle Systems* (McGraw-Hill, New York, 1971).

[32] M. Karolak, G. Ulm, T. Wehling, V. Mazurenko, A. Poteryaev, and A. Lichtenstein, J. Electron Spectrosc. Relat. Phenom. **181**, 11 (2010).

[33] I. V. Solovyev, Phys. Rev. B **73**, 155117 (2006).

[34] T. Miyake and F. Aryasetiawan, Phys. Rev. B **77**, 085122 (2008).

[35] J. M. Longo and P. Kierkegaard, Acta Chem. Scand. **24**, 420 (1970).

[36] O. K. Andersen and O. Jepsen, Phys. Rev. Lett. **53**, 2571 (1984); O. K. Andersen, Z. Pawlowska, and O. Jepsen, Phys. Rev. B **34**, 5253 (1986).

[37] O. K. Andersen and T. Saha-Dasgupta, Phys. Rev. B **62**, 16219 (2000).

[38] J. M. Tomczak, F. Aryasetiawan, and S. Biermann, Phys. Rev. B **78**, 115103 (2008).

[39] A. I. Poteryaev, J. M. Tomczak, S. Biermann, A. Georges, A. I. Lichtenstein, A. N. Rubtsov, T. Saha-Dasgupta, and O. K. Andersen, Phys. Rev. B **76**, 085127 (2007).

[40] J. M. Tomczak and S. Biermann, J. Phys. Condens. Matter **19**, 365206 (2007).

[41] H. J. Vidberg and J. W. Serene, J. Low Temp. Phys. **29**, 179 (1977).

[42] The value $V = 2$ eV was found to be the one that results in the best agreement with the CDMFT results and experimental band gap.

[43] J. Kunes and V. I. Anisimov, Phys. Rev. B **78**, 033109 (2008); M. Sentef, J. Kunes, P. Werner, and A. P. Kampf, *ibid.* **80**, 155116 (2009).

[44] J. P. Pouget, H. Launois, T. M. Rice, P. Dernier, A. Gossard, G. Villeneuve, and P. Hagenmuller, Phys. Rev. B **10**, 1801 (1974).

[45] M. Marezio, B. McWhan, J. P. Remeika, and P. D. Dernier, Phys. Rev. B **5**, 2541 (1972).

[46] J. P. Pouget, H. Launois, J. P. D'Haenens, P. Merenda, and T. M. Rice, Phys. Rev. Lett. **35**, 873 (1975).

[47] U. G. Nielsen, J. Skibsted, and H. J. Jakobsen, Chem. Phys. Lett. **356**, 73 (2002).

[48] J. P. D'Haenens, D. Kaplan, and P. Merenda, J. Phys. C **8**, 2267 (1975).

[49] K. A. Chao, J. Spalek, and A. M. Oles, J. Phys. C **10**, L271 (1977).